Golden Angle Radial Imaging for Improved Visualisation of Initial Stages of Inhalation in Dynamic ^{3}He Lung MRI

H. Marshall[1], **S. Ajraoui**[1], **and J. M. Wild**[1]
[1]Academic Unit of Radiology, University of Sheffield, Sheffield, South Yorkshire, United Kingdom

Introduction: The study of ventilation dynamics with hyperpolarised ^{3}He may provide insights into lung pathophysiology. Several sequences have been proposed to perform dynamic studies including EPI [1], spiral [2] and radial acquisitions [3-6], which enable fast imaging of the contrast uptake in the lungs. Standard radial acquisition increments the projection angle sequentially such that images can be successfully reconstructed from a pre-determined fixed number of projections. Flexible reconstruction of a dynamic dataset at any chosen spatio-temporal resolution is valuable in order to visualise the contrast uptake and adapt to the specific dynamics of a particular dataset. Multiple resolution radial imaging [7], where multiple angularly-undersampled radial datasets are interleaved over time such that higher resolution images can also be generated from their combination, goes some way towards achieving this goal. A similar strategy has been used to image the inhalation dynamics of a ventilated guinea pig by acquiring data over multiple respiration cycles [3]. In human ^{3}He lung MRI a radial acquisition strategy which added 90° to each successive sequential projection angle increment was used for a more uniform coverage of k-space [4]. Incrementation of projection angle by the golden angle (111.246°) provides a relatively uniform filling of k-space for any chosen temporal window, allowing a truly flexible reconstruction where images can be generated at any chosen spatio-temporal resolution [8]. Here golden angle radial sampling was used to image the inhalation of hyperpolarised ^{3}He in a healthy volunteer and the results were compared to those from sequential radial data acquisition.

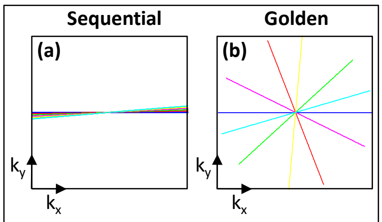

Fig 1: (a) sequential (θ=0.896°) and (b) golden (θ=111.246°) radial k-space sampling schemes shown for projections 1 to 6.

Methods: Experiments were conducted using a Philips 3T Intera system and data were processed in Matlab. A prototype Helmholtz coil of 20cm diameter loops was used for linear T-R. ^{3}He was polarised to ~25% with a Helispin polariser (GE).

<u>'Sequential' acquisition</u>: 250ml of hyperpolarised ^{3}He mixed with 750ml of N_2 was inhaled slowly by a healthy volunteer following the start of the imaging sequence, then held in the lungs for the remainder of the data acquisition. A thick coronal slice of the lungs (30cm slice, FOV = 380x380mm^2, k_r matrix:128, full echo, TR/TE: 5.4/2.3ms) was imaged using a 2D spoiled gradient echo (SPGR) sequence. Data were acquired using a radial sequence with 201 sequentially ordered projections per dynamic (θ=0.896°, meets Nyquist criterion in both r and θ) for 13 cycles (of 201 projections swept through 180°).

<u>'Golden angle' acquisition</u>: The above procedure was repeated, except that the data were acquired with a radial sequence where the projection angle was incremented by the golden angle (θ=111.246°) for 2560 successive projections. All other parameters remained the same.

Figure 1 shows an example of the radial projection acquisition order in k-space for the (a) sequential and (b) golden angle acquisition schemes. Data were reconstructed using regridding at multiple resolutions (angular undersampling factors); 32, 64, 96, 128, 164 and 201 projection reconstructions.

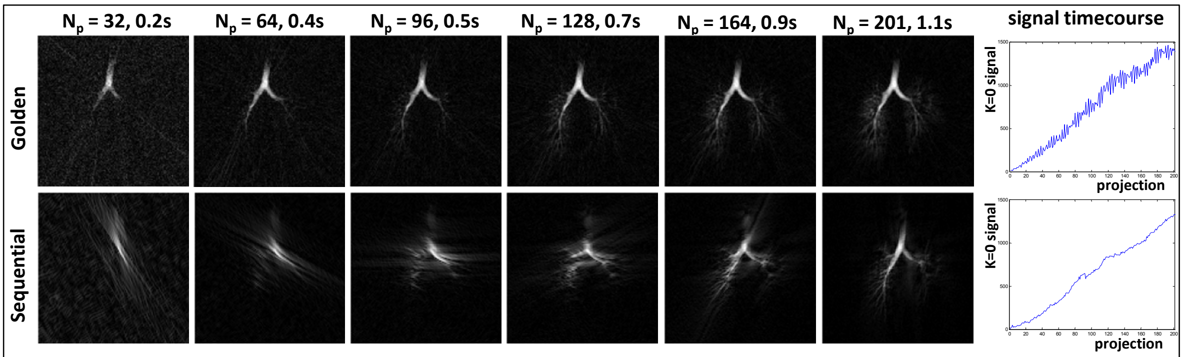

Fig 2: Reconstructions using different numbers of projections (N_p) starting from the beginning of contrast uptake, i.e. projections 1 to 32, projections 1 to 64 etc, for golden angle (top row) and sequential (bottom row) radial data. The plots (right column) show the signal time course from the centre of k-space projections 1 to 201 for golden angle (top) and sequential (bottom) data.

Results and Discussion: Figure 2 shows the first images of uptake of ^{3}He reconstructed at different resolutions (always starting from the first time point of ^{3}He signal) for the golden angle (top row) and sequential data (bottom row). The sequential data acquisition can only provide images reconstructed with the number of projections prescribed in the acquisition (201 projections for this data, which meets the Nyquist criterion for k_r=128). The golden angle data acquisition allows adaptive, multi-resolution reconstructions of the first stages of inhalation (figs 2 and 3). The high level of angular undersampling results in streaking artifacts but affords fast temporal resolution with which to visualise the inhalation process. The random nature of the undersampling artifacts produced by the golden angle radial acquisition could make it particularly suitable for compressed sensing [9] reconstruction. Future work will include the use of k-space trajectory mapping [10] to correct for any reconstruction errors due to an imperfect k-space trajectory which results from the harder switching in gradient amplitude from projection to projection in the golden angle scheme.

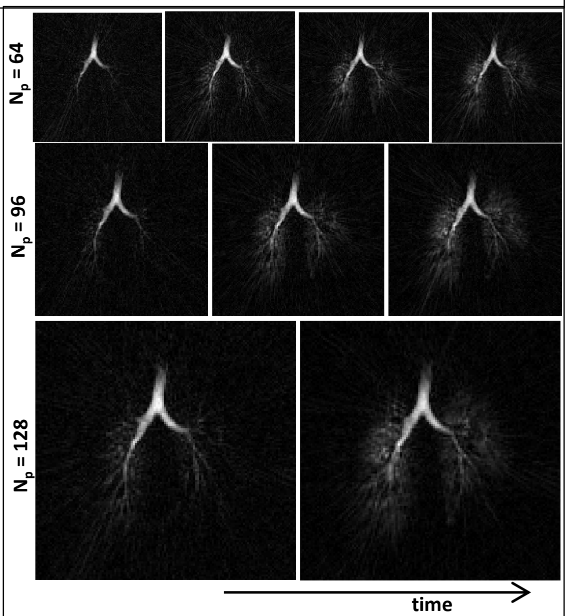

Fig. 3: multi-resolution reconstruction of golden angle radial data, top row = 64 projections, middle row = 96 projections, bottom row = 128 projections

Conclusions: Golden angle radial data acquisition allows visualisation of the initial hyperpolarised ^{3}He inhalation stages and flexible reconstruction of dynamic lung images at any spatiotemporal resolution.

Acknowledgements: GE for polariser support, EPSRC grant #EP/D070252/1, and Rachel Chan for regriddding code.

References: [1] Saam et al, MRM 42:507-514 (1999); [2] Salerno et al, MRM 46:667-677 (2001); [3] Viallon et al, MRM 41:787-792 (1999); [4] Wild et al, MRM 49:991-997 (2003); [5] Holmes et al, JMRI 26:630-636 (2007); [6] Holmes et al, MRM 59:1062-1071 (2008); [7] Song et al, MRM 46:503-509 (2001); [8] Winkelmann et al, IEEE Trans Med Imaging 26:68-76 (2007); [9] Lustig et al, MRM 58:1182-1195 (2007); [10] Duyn et al, JMR 132:150-153 (1998).